

Validity of Mutual Inductor Model for Electromagnetic Coupling between Vias in Integrated-Circuit Packages and Printed Circuit Boards

Jin Zhao and Jiayuan Fang
 Department of Electrical Engineering
 State University of New York at Binghamton, Binghamton, NY 13902
 Email: jzhao@binghamton.edu, fangj@binghamton.edu

Abstract

A validity study of mutual inductor model for electromagnetic coupling between vias in integrated-circuit packages and printed circuit boards is presented in this paper. The procedure of extracting mutual inductor model between vias is demonstrated. Then the validity of the mutual inductor model is studied by comparing the solution from the mutual inductor model with that from the full-wave field simulation. It is found that the validity frequency range of the mutual inductor model is mostly determined by the lowest resonant frequency of the package structure.

Introduction

With ever-increasing IC speed and packaging density, electrical modeling and simulation of electronic packages have become one of the critical issues in overall system design. Improperly designed packages lead to signal integrity degradations such as signal delay, crosstalk, and ground noise, which limit the overall system performance. Electromagnetic coupling inside a package structure is mostly between traces and vias. There have been many studies in past decades on models for coupling between traces. However, it has been shown that coupling between vias, especially for multi-layered IC packages and printed circuit boards, can be even more significant than the coupling between traces [1]. Therefore, accurate signal integrity analysis can not be achieved without adequate models for coupling between both vias and traces.

The electromagnetic coupling between vias has often been modeled by mutual inductance between vias [2-3]. It is known that the mutual inductor model is a low frequency approximation. This model does not take into account the wave propagation delay between vias, nor resonance inherent in multi-layered metal plane structures.

In this paper, the mutual inductor model is reviewed first, and then the circuit models for several different package structures are given as examples. The procedure of extracting the mutual inductor model is demonstrated. It will be shown through numerical examples that, with the mutual inductor model, simulation results are acceptable for low frequency signals but contain increasingly significant error as signal frequency becomes higher. Since the mutual inductor model does not include the effects of wave propagation delay between vias, the validity of the mutual inductor model also depends on the distance between vias. However, electronic packages have resonance at various frequencies, the mutual inductor model becomes totally invalid near and above the first resonant frequency of the package structure.

Mutual Inductor Model of Coupling between Vias

With the mutual inductor model, the coupling between vias is modeled by a mutual inductor [3]. Let's first consider a simple structure shown in Fig. 1. It is assumed that at the location of the reference via, the power and the ground planes are connected to an ideal power supply. A shorting via connecting the two metal planes is actually used in present example to represent the zero impedance of the ideal power supply. We can consider that the current I_1 flows through the path that includes via₁, power and ground planes, and the reference via. The self-inductance associated with this path is represented by L_{11} in Fig. 2. The current I_2 flows through the path that includes via₂, the power and ground planes, and the reference via. The corresponding self-inductance of this path is represented by L_{22} . The coupling between via₁ and via₂ is modeled by a mutual inductor L_{12} representing the magnetic flux linkage between two current loops.

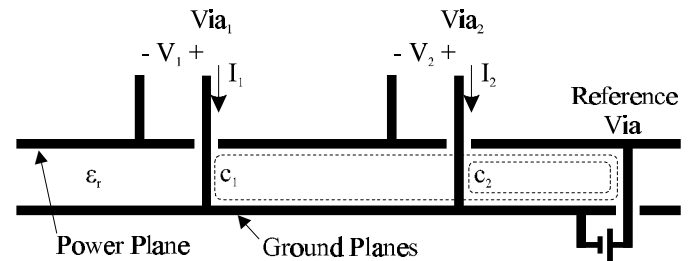


Figure 1. Coupling between two vias in a package

In the lumped circuit model shown in Fig. 2, the capacitor C represents the capacitance between two metal planes. When the two metal planes are connected to an ideal power supply with zero input impedance, the capacitor C has practically no effect.

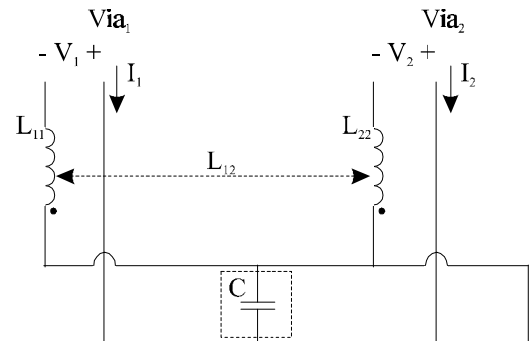


Figure 2. Lumped inductor model representing vias and via coupling in package

The above procedure of generating lumped inductor model for vias between metal planes can be extended to more

general configurations. Fig. 3 shows that there are n vias between the two metal planes. Choose one of the vias, via n , as the reference via. The lumped circuit model of the configuration shown in Fig. 3 is displayed in Fig. 4. The inductor L_{ii} represents the self-inductance of the current loop consisted of via $_i$, the power and ground planes, and the reference via. The mutual inductor L_{ij} represents the coupling between the corresponding two current loops.

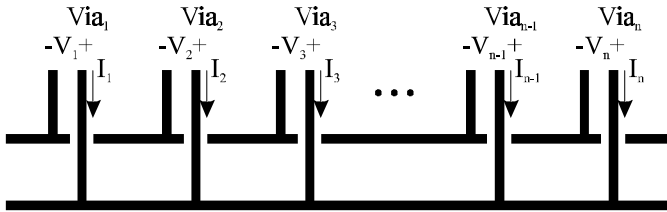


Figure 3. Coupling between n vias in a package

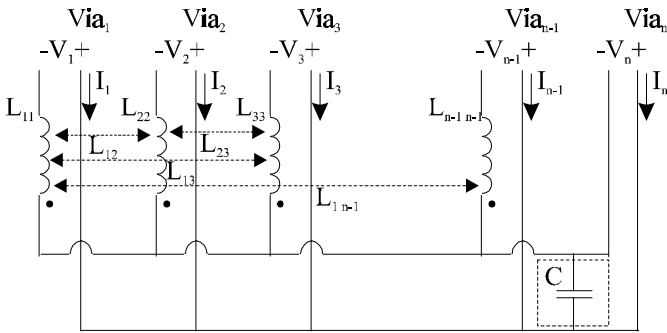


Figure 4. Lumped inductor model representing vias and via coupling in the package shown in Fig. 3.

Fig. 5 shows another configuration where vias are connected to the external circuits above and below the two metal planes. Choose one of the vias, e.g. via $_5$, as the reference via. The lumped inductor model for the configuration in Fig. 5 is shown in Fig. 6.

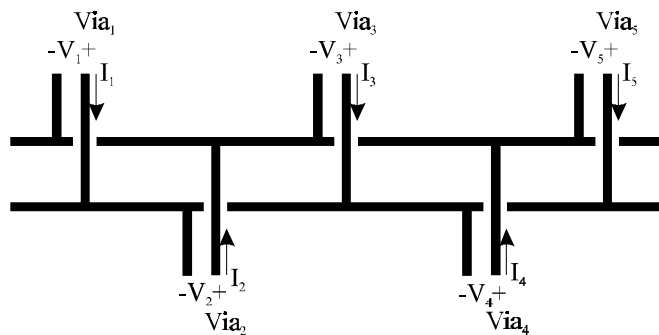


Figure 5. Vias connected to circuits both above and below the two metal planes

It can be shown, which is not to be discussed here but will appear in a separate publication, that the above procedure of generating lumped via coupling models can be extended to structures of more than two metal planes.

Numerical Extraction of Lumped Inductor Model

The numerical extraction of the lumped inductor model is illustrated by the following example. The structure of the example is shown in Fig. 7. Fig. 7(a) is the top view of the structure. The power and ground planes are 10 cm by 10 cm in size. The separation between the two planes is 500 μ m. The dielectric constant of the medium between the two planes is 4.0. With the origin chosen at the lower left corner of structure, Via $_1$ is located at (4.5 cm, 5.0 cm), Via $_2$ at (5.5 cm, 5.0 cm). The via connected to the ideal power supply, and chosen to be the reference via, is located at (9.5 cm, 5.0 cm).

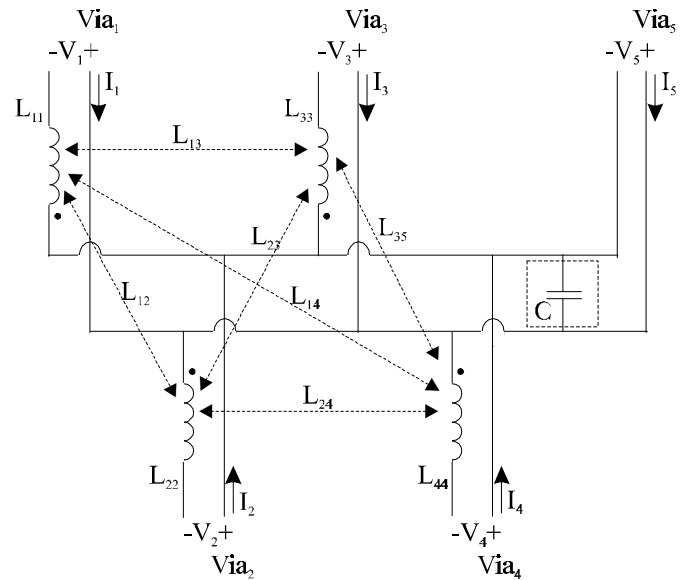


Figure 6. Lumped inductor model representing vias and via coupling in the package shown in Fig. 5

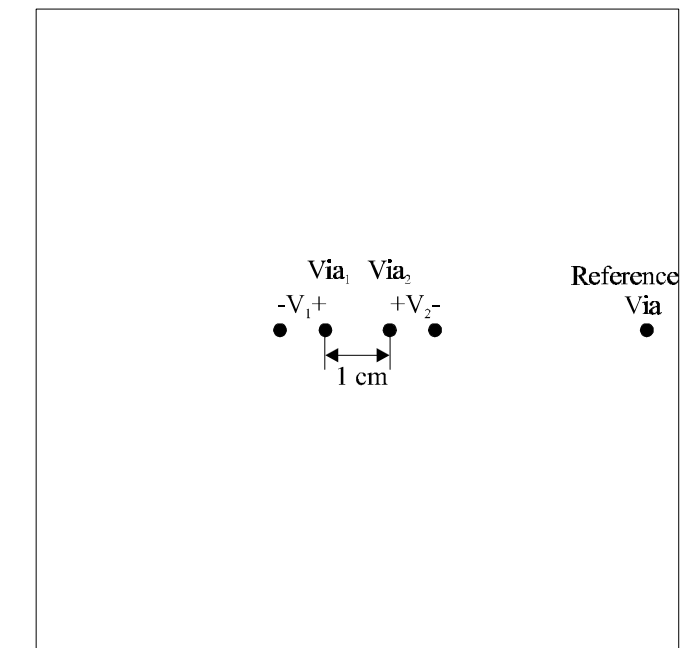


Figure 7(a). Top view of the package

Fig. 7(b) shows the side view of the structure and the connection between circuits and vias. One pair of vias, which include via₁, is connected to a current source in parallel with a 2 Ω resistor. The other pair of vias is opened-circuited but is modeled by being connected to a 10 MΩ resistor. The lumped inductor model for the configuration of Fig. 7 is shown in Fig. 8.

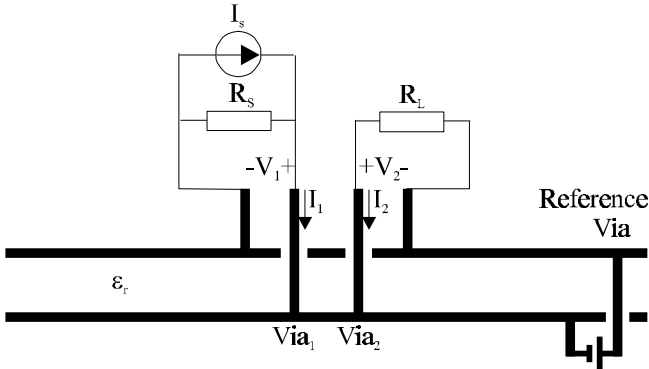


Figure 7(b). Side view of the package and connection between circuits and vias

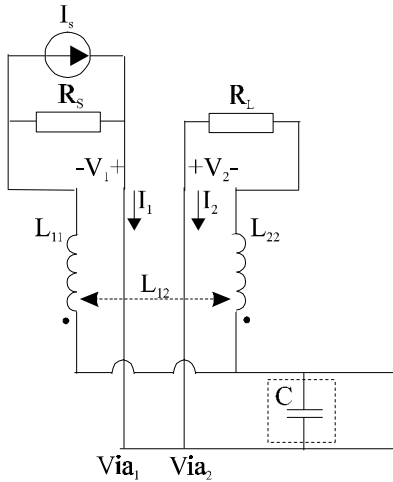


Figure 8. The lumped inductor model and circuit connection of the package configuration shown in Fig. 7

A full wave electromagnetic tool [4] is used to extract the lumped inductor model. The waveform of the current source I_S is a Gaussian pulse. In the simulation, voltages $V_1(t)$, $V_2(t)$ and the current $I_1(t)$ that flows in Via₁ are recorded. For the present case, the current $I_2(t)$ can be regarded as zero. The self-inductor L_{11} and mutual inductor L_{12} can be calculated by

$$L_{11} = \lim_{f \rightarrow 0} \operatorname{Im} \left[\frac{V_1(f)}{I_1(f) 2\pi f} \right] \Bigg|_{I_2=0} \quad (1)$$

$$L_{12} = L_{21} = \lim_{f \rightarrow 0} \operatorname{Im} \left[\frac{V_2(f)}{I_1(f) 2\pi f} \right] \Bigg|_{I_2=0} \quad (2)$$

where $V_1(f)$, $V_2(f)$ and $I_1(f)$ are the Fourier transforms of $V_1(t)$, $V_2(t)$ and $I_1(t)$.

The self-inductor L_{22} can be calculated similarly. Connect the current source and the parallel resistor R_S to the pair of vias that include Via₂, and connect the 10 MΩ resistor R_L to the pair of vias that include Via₁; do the simulation again. Now current $I_1(t)$ is zero, and the self-inductor L_{22} can be found by

$$L_{22} = \lim_{f \rightarrow 0} \operatorname{Im} \left[\frac{V_2(f)}{I_2(f) 2\pi f} \right] \Bigg|_{I_1=0} \quad (3)$$

Fig. 9 displays the self-inductor L_{11} , L_{22} and the mutual-inductor L_{12} as a function of frequency. The inductance values in the lumped circuit model are the low frequency limits of the inductances displayed in Fig. 9, which are found to be $L_{11} = 1.1656$ nH, $L_{22} = 1.0887$ nH, and $L_{12} = 0.7465$ nH.

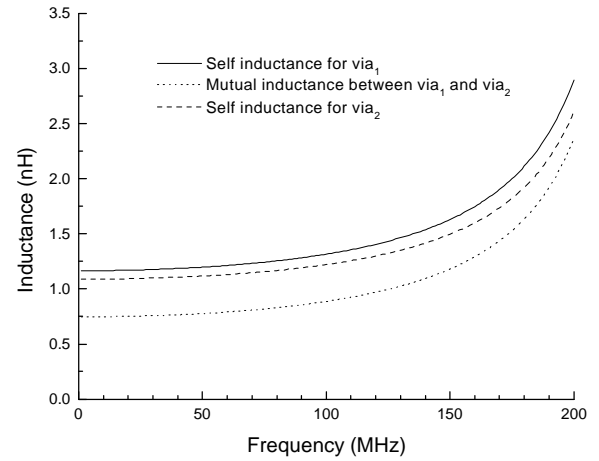


Figure 9. Extracted self and mutual frequency-dependent inductances

Comparison between Full-Wave Field Simulation and Lumped Circuit Simulation

In this section, the full-wave field simulation and the lumped circuit simulation are compared with excitations of Gaussian signals with different pulse widths. For the full-wave field simulation, the connection between circuits and vias is the same as that shown in Fig. 7(b). The circuit shown in Fig. 8 is used for the lumped circuit simulation.

In the first comparison, the pulse width of a Gaussian signal is 5 ns. Fig. 10(a) shows that the voltage across R_L obtained by the full-wave field simulation and that obtained from the lumped circuit simulation by using the mutual inductor model agree well.

Then the pulse width of the Gaussian signal is reduced to 500 ps. Fig. 10(b) shows the results from different simulations. As one can see that the voltage obtained from the lumped circuit simulation by using the mutual inductor model is quite different to that obtained by the full-wave field simulation, which shows that the mutual inductor model is totally unacceptable.

These results show that the frequency-independent mutual inductor model is only valid when frequency is very low or the spectrum of the signal is very low. When the frequency or

the spectrum of the signal is high, the mutual inductor model becomes invalid. This can also be seen in Fig. 11, which shows the ratio of V_2 and I_1 as a function of frequency.

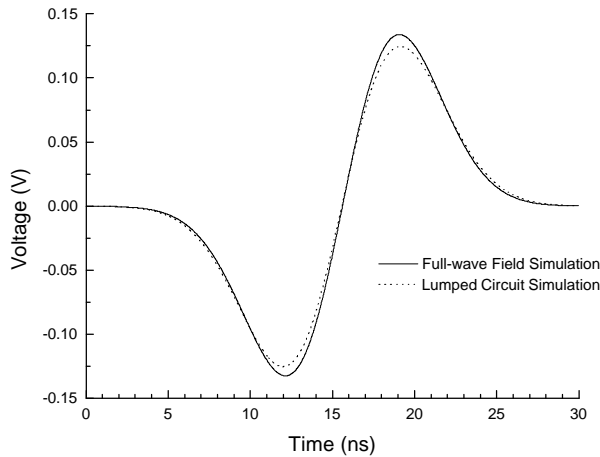


Figure 10(a)

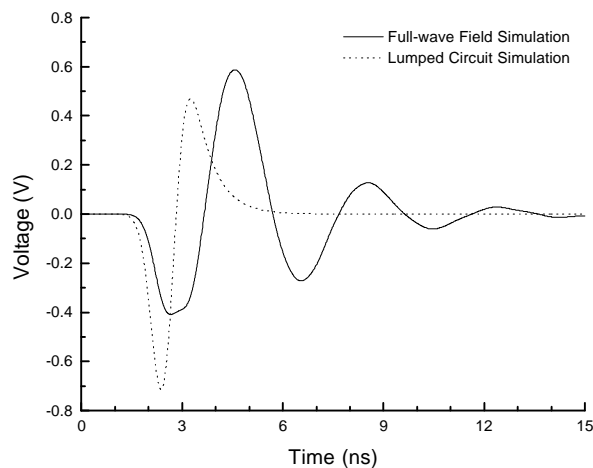


Figure 10(b)

Figure 10. Comparison of induced voltage across the load R_L shown in Fig. 7(b) obtained by full-wave field simulation and that from lumped circuit simulation by using mutual inductor model when (a) the pulse width is 5 ns, and (b) the pulse width is 500 ps.

Package Resonance and Validity of Mutual Inductor Model

Due to reflections from edges of metal planes, resonance can happen inside packages and large input impedance values will appear around resonant frequencies. Let's consider the package consists of two metal planes separated by 500 μm . The plane is 10 cm by 10 cm in size. The dielectric constant of the medium between two metal planes is 4.0. Fig. 12 is the top view of the package. The input impedance at the location of Via_1 and the coupling between Via_1 and Via_k ($k = 2, \dots, 6$) are studied by using the full wave electromagnetic tool [4]. The input impedance at location of Via_1 and the transfer

functions of $V_k(f)$ over $I_1(f)$ ($k = 2, \dots, 6$) are shown in Fig. 13. One can see that their values become very large at $f_r = 153$ MHz, which is the lowest resonant frequency of the package. Fig. 14 shows the effective mutual inductances for via coupling between Via_1 and Via_k ($k = 2, \dots, 6$). At the zero frequency limit, the values of the mutual inductances are: $L_{12} = 2.924$ nH, $L_{13} = 1.988$ nH, $L_{14} = 1.738$ nH, $L_{15} = 1.542$ nH, and $L_{16} = 0.695$ nH. Fig. 14 also shows the relative errors of the mutual inductances at different frequencies to the values at zero frequency. The relative error is about 5 % at $0.2 f_r$, which is 31 MHz and about 35 % at $0.5 f_r$, which is 76 MHz.

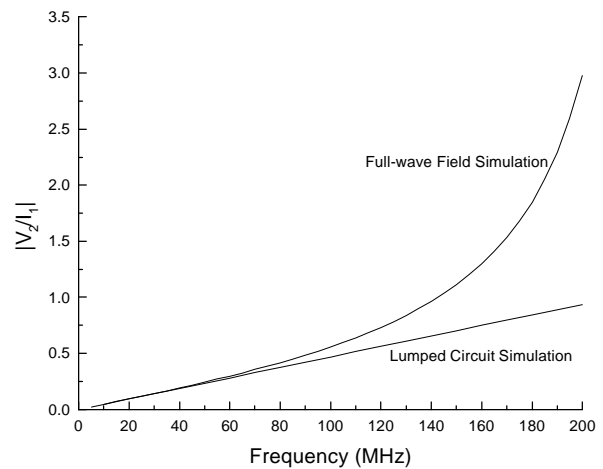


Figure 11. Comparison between results from lumped circuit simulation by using mutual inductor model and full-wave field simulation

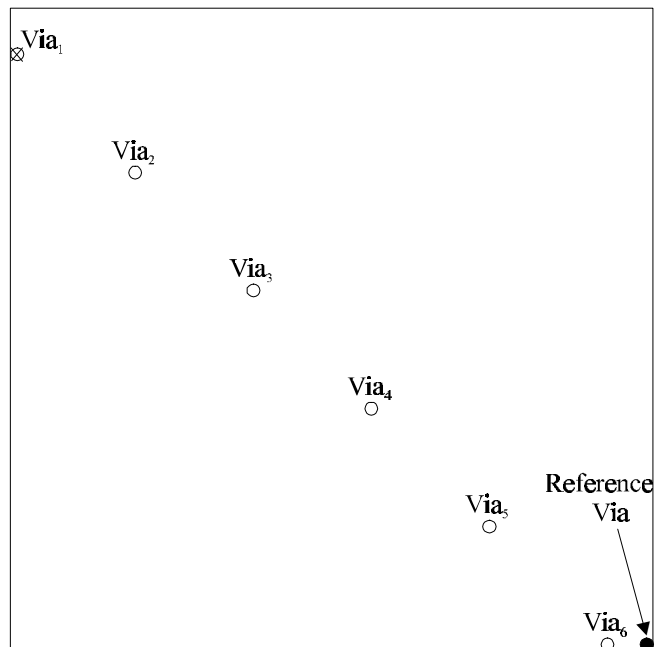


Figure 12. Top view of the package

As the frequency moves closer to the resonant frequency, the zero-frequency mutual inductor model becomes less valid.

The lowest resonant frequency of a package can be moved to higher frequency by adding shorting via array [5]. The next example shows that this has the same effects on the validity of the mutual inductor model. After adding shorting via array, the package shown in Fig.12 is redrawn in Fig. 15. Again, it is assumed that the upper metal plane is connected through vias and an ideal power supply to the lower metal plane. The resonance of the package is studied first. Fig. 16 shows the input impedance at location of Via₁ and the transfer functions of $V_k(f)$ over $I_1(f)$ ($k = 2, \dots, 12$). The lowest resonant frequency is now moved to 2.025 GHz, which is much higher than the previous one at 153 MHz. The frequency-dependent mutual inductances for via coupling between Via₁ and Via_k ($k = 2, \dots, 12$) are shown in Fig. 17. At zero frequency, the values of mutual inductances are: $L_{12} = 141.9$ pH, $L_{13} = 48.25$ pH, $L_{14} = 21.34$ pH, $L_{15} = 8.307$ pH, $L_{16} = 3.947$ pH, $L_{17} = 1.606$ pH, $L_{18} = 0.787$ pH, $L_{19} = 0.328$ pH, $L_{110} = 0.163$ pH, $L_{111} = 0.016$ pH, and $L_{112} = 0.003$ pH.

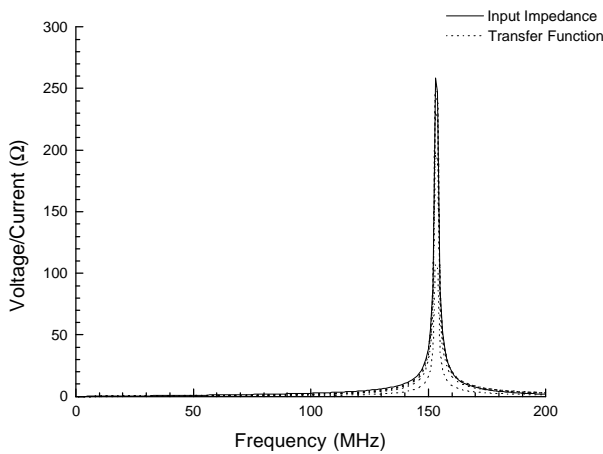


Figure 13. Voltage over current as a function of frequency at different via location

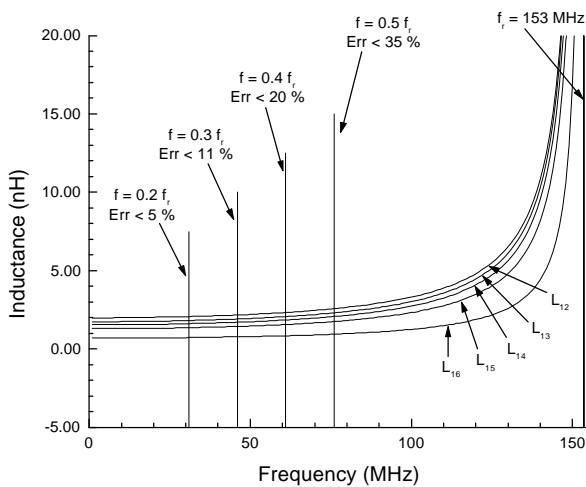


Figure 14. Extracted mutual frequency-dependent inductance

Fig. 17 also shows the relative errors of the mutual inductances at different frequencies to the value at zero frequency. Table 1 lists the data for the relative error curves in Fig. 17. One can see that the validity frequency range for near via coupling is higher than that for far via coupling. Meanwhile, the mutual inductance of far via coupling is much smaller than that of near via coupling, and therefore may be neglected. The shorting via array has moved the resonance to higher frequency, at same time, it also reduces the coupling between vias.

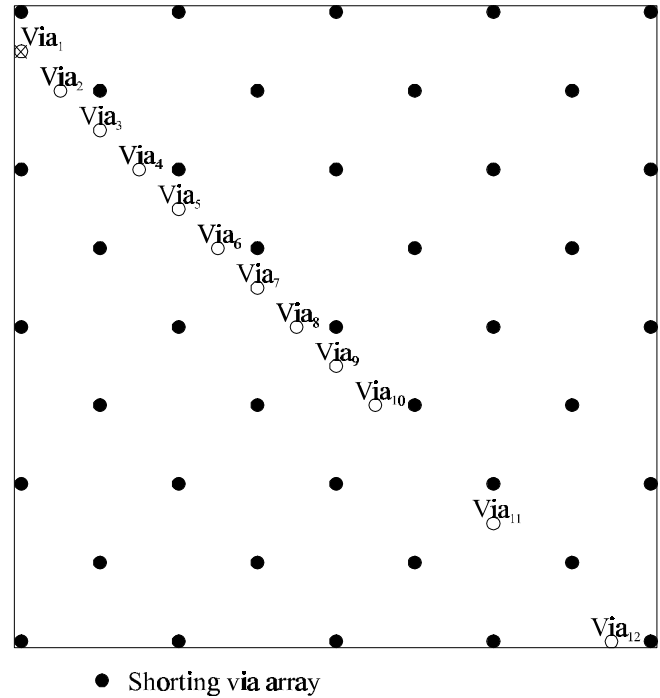


Figure 15. Top view of the package with shorting via array

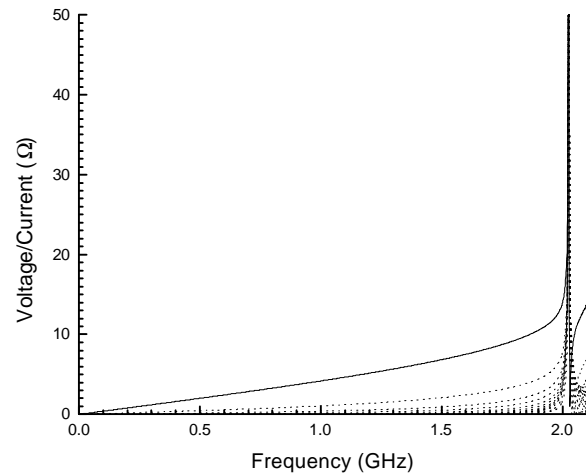


Figure 16. Voltage over current as a function of frequency at different via location

With above study, one can see that the lowest resonant frequency of the package is the main limitation of the validity of mutual inductor model.

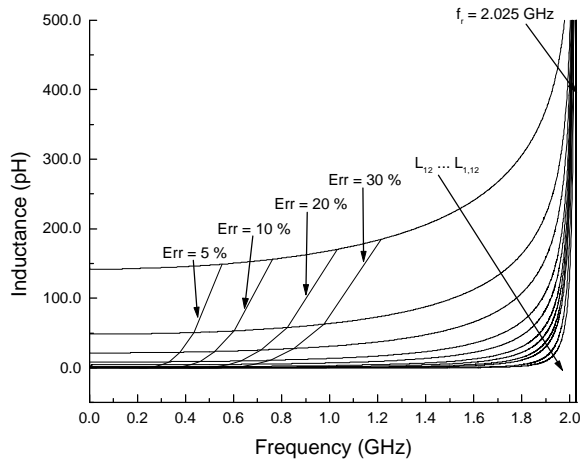


Figure 17. Extracted mutual frequency-dependent inductance

Table 1. Frequency of mutual inductance with different relative error (MHz)

Inductance (pH)	Freq. with 5 %	Freq. With 10 %	Freq. with 20 %	Freq. with 30 %
L ₁₂ =141.9	553	763	1032	1212
L ₁₃ =48.25	435	604	824	977
L ₁₄ =21.34	376	522	716	851
L ₁₅ =8.306	331	461	633	755
L ₁₆ =3.946	301	421	580	692
L ₁₇ =1.606	274	386	532	636
L ₁₈ =0.7857	257	361	499	596
L ₁₉ =0.3273	239	337	467	559
L _{1 10} =0.1629	226	319	443	531
L _{1 11} =0.01567	180	264	377	453
L _{1 12} =0.003179	127	208	328	414

Conclusion

With the study presented by this paper, it is shown that, with the mutual inductor model, simulation results are acceptable for low frequency signals. However, the model is not acceptable when signal frequency becomes higher. Especially the mutual inductor model becomes totally invalid near and above the lowest resonant frequency of the package structure. For a given package, the resonant frequency and the frequency limitation of the mutual inductor model can be found through the full wave electromagnetic tool.

Acknowledgment

The work is supported in part by the National Science Foundation under grant MIP-9357561, the Integrated Electronics Engineering Center at the State University of New York at Binghamton, and the Advanced Research Projects Agency under grant F49620-96-1-0341.

References

1. J. Zhao and J. Fang, "Significance of Electromagnetic Coupling through Vias in Electronics Packaging," IEEE 6th Topical Meeting on Electrical Performance of Electronic Packaging, Conference Proceedings, pp. 135-138, Oct. 27-29, 1997, San Jose, CA.
2. E. Davison, G. A. Katopis and T. Sudo, "Package Electrical Design," Chapter 3, Microelectronics Packaging Handbook, second edition, edited by R. R. Tummala, E. J. Rymaszewski and A. G. Klopfenstein, Chapman & Hall, 1997.
3. W. Becker, B. McCredie, G. Wilkins, and A. Iqbal, "Power Distribution Modeling of High Performance First Level Computer Packages," IEEE 2nd Topical Meeting on Electrical Performance of Electronic Packaging, Conference Proceedings, pp. 203-205, Oct.20-22, 1993.
4. Information on SPEED 97, which is produced by SIGRITY, can be found from www.sigritty.com
5. J. Fang, J. Zhao and J. Zhang, "Shorting Via Arrays for the Elimination of Package Resonance to Reduce Power Supply Noise in Multi-layered Area-array IC Packages," IEEE symposium on IC/Package Design Integration, Feb. 2-3, 1998, Santa Cruz, CA.